6th International Symposium on Hydraulic Structures Portland, Oregon, USA, 27-30 June 2016
Hydraulic Structures and Water System Management
ISBN 978-1-884575-75-4 DOI: 10.15142/T330628160857

Effect of a Deflector Aerator on Stepped Spillway Flow

S. Terrier[1], M. Pfister[1] and A.J. Schleiss[1]
[1]Laboratory of Hydraulic Constructions (LCH)
École polytechnique fédérale de Lausanne (EPFL)
Station 18, CH-1015 Lausanne
Switzerland
E-mail: stephane.terrier@epfl.ch

ABSTRACT

Systematic physical model tests are performed on a stepped spillway equipped with a bottom aerator at the beginning of the stepped part. A deflector is used to issue a jet in order to initiate air entrainment into the flow. A horizontal slot located in the vertical face of the first step allows for air supply underneath the flow. The cavity subpressure was measured to ensure optimal aerator performance, namely atmospheric pressure conditions. The air discharge entrained below the jet is measured to derive the aerator air entrainment coefficient. The local air concentrations are spatially measured downstream of the aerator at regularly spaced profiles, allowing the investigation of air transport and detrainment as well as the average and bottom air concentrations. The present paper focuses on the resulting spatial distribution of air concentration for five deflector geometries. The chute angle, step height, approach flow Froude number, and approach flow depth were kept constant so that the differences occur mostly on the jet length and air entrainment coefficient. The flow depth and the air concentration rapidly converge towards quasi-uniform flow values downstream of the aerator.

Keywords: *aerator, air concentration, air entrainment, cavitation, deflector, stepped spillway*

1. INTRODUCTION

Chute aerators are installed to prevent cavitation damages, and they were studied in detail on *smooth* bottom spillways in terms of global air entrainment coefficient (Koschitzky 1987; Chanson 1988; Rutschmann 1988; Skripalle 1994; Kökpinar and Göğüş 2002) as well as streamwise air transport (Kramer 2004; Pfister 2008).

In parallel, *stepped* spillways have become widespread in the past decades. Research has shown that stepped spillways may be endangered by cavitation even more than smooth spillways, particularly for high, specific discharges. The most critical location is just upstream of the self-aeration at the inception point, with already high velocities. Pressure investigations on the upper part of the vertical face of steps showed that a flow velocity higher than 15 m/s could cause cavitation, which would limit the specific discharge to q = 14 m^2/s for a chute angle φ = 51.3 ° and a step height s = 1.2 m (Amador et al. 2009). Using acoustic measurements in a reduced ambient pressure facility, a critical cavitation index σ_c = 0.3–0.4 was obtained for a chute angle φ = 21.8 ° and σ_c = 0.60–0.65 for φ = 68.2 ° (Frizell et al. 2013). This is significantly higher than the critical value of σ_c = 0.2 for smooth chutes (Falvey 1990) and leads to specific discharges around q = 15 m/s at the inception point (Pfister and Boes 2014). As a consequence, besides issues of energy dissipation, the specific discharge of stepped spillways is usually limited to lower values than on smooth spillways. In order to overcome that limitation, flow aeration – mainly at the beginning of the chute – is necessary. However, Chanson (2015) questions the increased cavitation risk on stepped chutes.

Until now, only preliminary studies exist for the design of such aerators. Stepped chute aerators were first studied by Pfister et al. (2006a; b) and Schiess Zamora et al. (2008) for fixed aerator geometries, and only the discharge was varied. A comparison of smooth and stepped chute aerators was presented by Terrier et al. (2015).

2. PHYSICAL MODEL TESTS

Tests were performed on a physical model at the Laboratory of Hydraulic Constructions of EPFL. The channel has a streamwise length of 8.0 m, a width of 0.5 m, and an adjustable bottom angle φ (Figure 1). A jetbox generates the transition between the pressurized flow of the water supply system to a free surface flow in the channel. Unlike a standard ogee, it allows the independent variation of the approach flow depth h_o and Froude number $F_o = u_o/(gh_o)^{0.5}$, with u_o = approach flow velocity and g = gravity acceleration. Unit discharges up to $q = 0.486$ m^2/s are supplied. At the exit of the jetbox, the channel bottom is smooth for 0.47 m. Thereafter, sixty steps with a height of $s = 0.06$ m follow. The step height can be halved by adding inserts. The transition point between the two bottom surfaces is the origin of the coordinates x and z.

The aerator is located at the transition between the smooth and the stepped bottom. It consists of a deflector and an air supply system providing air into the first step. There is no offset between the upper smooth chute bottom and the pseudo-bottom of the stepped chute. The deflector is characterized by its angle α and its height t. The deflector lip is located at the coordinate $x = 0$. Air is supplied to the nappe below the jet through a 0.02 m high transversal slot in the vertical face of the first step. An airtight chamber with wide dimensions to avoid head losses – which would influence the jet length – is feeding the nappe. Air enters the chamber through a circular duct.

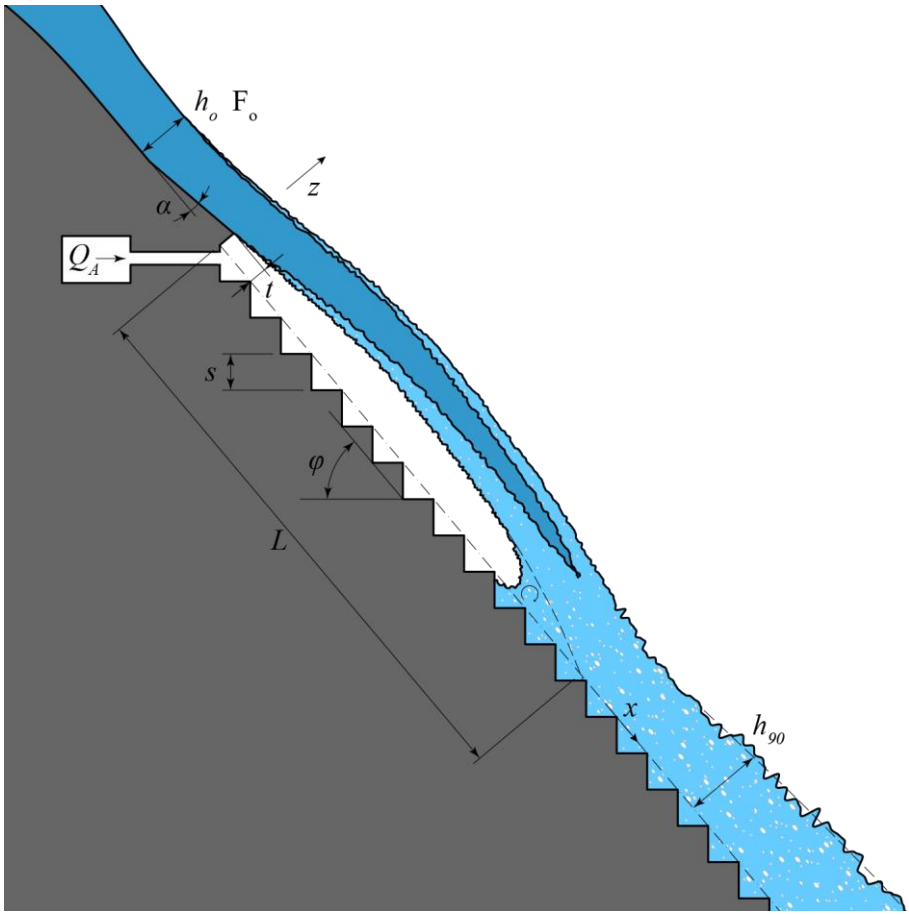

Figure 1. Definition sketch: approach flow depth h_o, approach flow Froude number F_o, deflector angle α, deflector height t, chute angle φ , step height s, jet length L and flow depth h_{90}

The air velocity is measured in the center of the air duct with a thermoelectric anemometer (Schiltknecht, Switzerland). The air discharge q_A is calculated by integrating the logarithmic velocity profile after verifying that the flow is turbulent in the air duct. A dual-tip fiber optical probe (RBI Instrumentation, France) is used to measure local

air concentrations in the flow. It is based on the different refraction index between air and water phases and uses a sampling rate of 1 MHz. The probe is fixed on an automatic positioning system that allows movement along the streamwise axis x and the depth axis z. Profiles are measured along the channel at regularly spaced intervals. A profile consists of 25 points, each measured during 20 s. All profiles start at a step edge with the closest point at $z \approx 0.003$ m. A U-shaped glass manometer is used to measure the air cavity subpressure Δp and verify that it does not affect the jet or the air entrainment. The effect of subpressure remains small if $\Delta p/h_o < 0.10$ (Tan 1984; Chanson 1988; Rutschmann 1988; Pfister 2011), and this criteria was satisfied with a maximum subpressure $\Delta p/h_o = 0.03$.

To systematically investigate stepped spillways aerators, six parameters are varied: the chute parameters φ and s, the flow parameters F_o and h_o, and the deflector parameter α and t (Figure 1). References tests without an aerator are performed to assess the relative effect of the aerator compared to the situation without an aerator. The results of the reference tests are similar to the stepped spillways literature. Herein, only the variation of the deflector parameters is presented (Table 1). The other parameters were kept constant with $\varphi = 30$ °, $s = 0.06$ m, $F_o = 5.5$, and $h_o = 0.075$ m.

Two-phase flows are sensitive to scale effects. Under the Froude similitude, the viscous force represented by the Reynolds number $R_o = u_o h_o/\nu$ is underestimated, and the surface tension force represented by the Weber number $W_o^{0.5} = u_o/(\sigma_w/\rho h_o)^{0.5}$ is overestimated, with ν = kinematic viscosity, σ_w = surface tension, and ρ = density. The tests presented herein all have the same approach flow condition with $R_o = 3.5 \cdot 10^5$ and $W_o = 153$, which respects the recommendations to limit scale effects related to the air concentration (Pfister and Chanson 2014).

Table 1 – Deflector geometry of the tests presented given, the deflector angle α, deflector height t, as well as he measured jet length L, air entrainment coefficient $\beta = q_A/q$ and cavity subpressure $\Delta p/h_o$

Test	α [°]	t [m]	L [m]	β [-]	$\Delta p/h_o$
R	-	-	-	-	-
A15	9.46	0.015	0.86	0.080	0.01
A30	9.46	0.030	1.22	0.124	0.01
B15	14.04	0.015	1.23	0.127	0.01
B30	14.04	0.030	1.63	0.160	0.01
B45	14.04	0.045	1.85	0.193	0.03

3. RESULTS

3.1. General Observations and Water Depth

Figure 2 shows photos of the upper channel half. The smooth bottom reach and the deflector can be seen on the left; the jetbox is outside of the picture. The reference test shows a progressive roughening of the surface without air entrainment in the first part. The surface inception point occurs shortly after the start of the stepped part near the 8th step. The streamwise position of the inception point oscillates with time. Downstream of the latter, the flow becomes white and aerated. The surface is irregular, and some spray is visible.

Aerated tests reveal that both jet surfaces become white and, thus, aerated. The jet has a regular and stable trajectory. Downstream of the impact, some spray with irregular splashing is visible. The splashing can reach the height of the jet.

The spatial air concentration field reveals the amount of air entrained (Figure 3). Apparent “steps” in the jet results from the interpolation code and are not physically based. This applies also for the sudden increase and decrease of concentration in the jet core at $x = 1.35$ for tests B30 and B45. The reference test indicates a surface inception at $x \approx 1.0$ m, with a high increase of air entrainment close to the surface but much slower at the bottom.

For aerated tests, the thickness of the jet blackwater core progressively decreases with the length, and an air concentration of $C > 0.10$ is rapidly attained. A rapid evolution of air concentration occurs at the jet impact. The bottom air concentration decreases as a result of the impact pressure. Tests A30, B15, and B30 show a kind of bottom roller before the jet impact. Downstream of the impact, there is a gradual variation of the air concentration tending to equilibrium. The spray previously observed is not detected.

The flow depth z_{90} is defined by the depth where $C = 0.90$. For the reference test, z_{90} gradually increases as the flow becomes progressively aerated (Figure 4). Surface inception – at $x \approx 1$ m – causes a higher increase in the flow depth before it stabilizes at a value of $z_{90} = 0.111$ m. The jet lifts the water surface of the aerated tests in the first part of the channel. The depth at the impact is highly similar to the depth of the reference test at the same location. Downstream of the impact, the water level is stable at a level similar to the reference test. There is a slight oscillation of the surface, which is particularly apparent for tests B30 and B45 with the longer jets. The flow depth at the end of the channel is consistent with the value of 0.114 m according to Boes and Hager (2003).

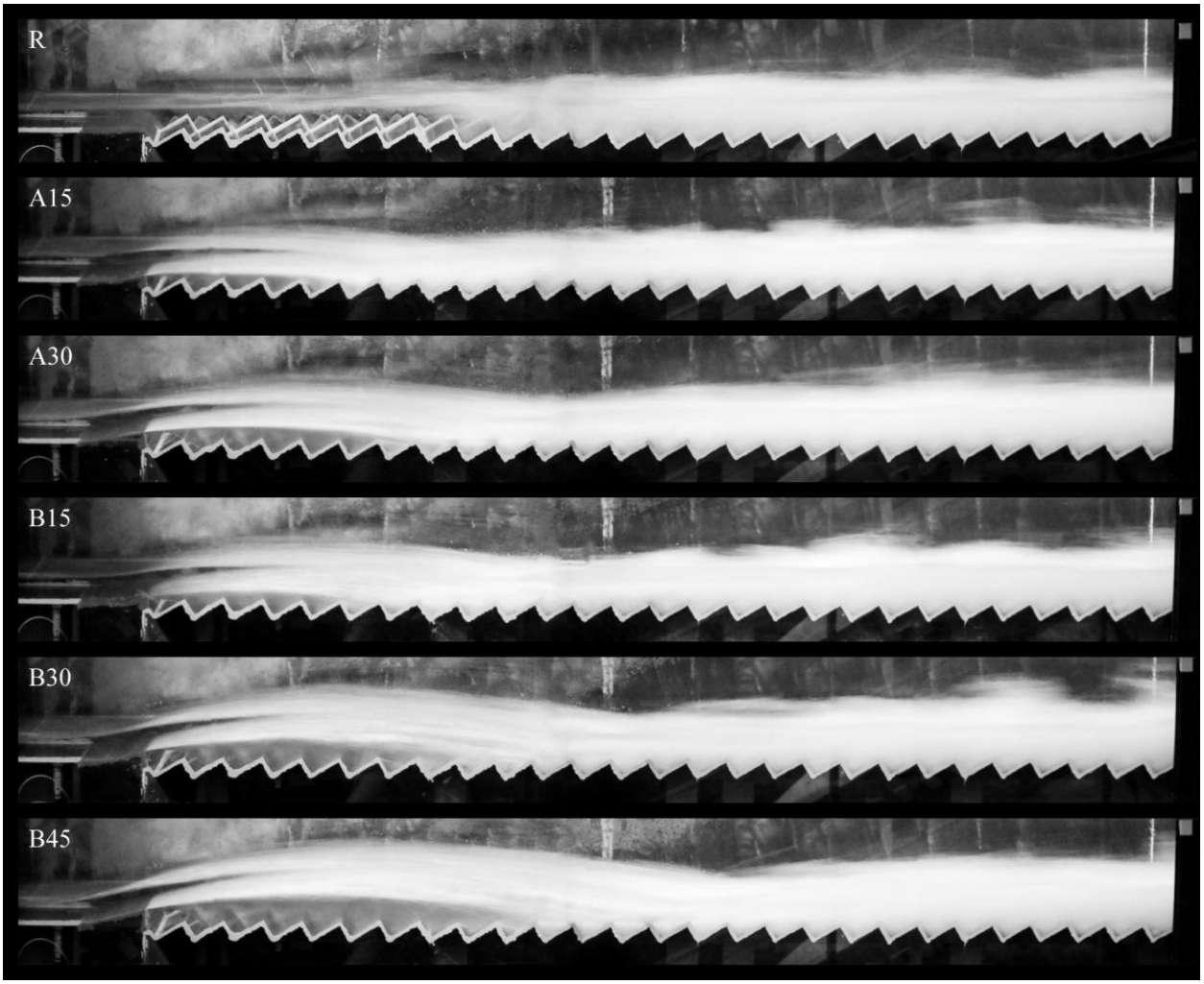

Figure 2. Photos of the upper channel flow for reference test R without aerator, and tests A15, A30, B15, B30, and B45 with aerator (cf. Table 1)

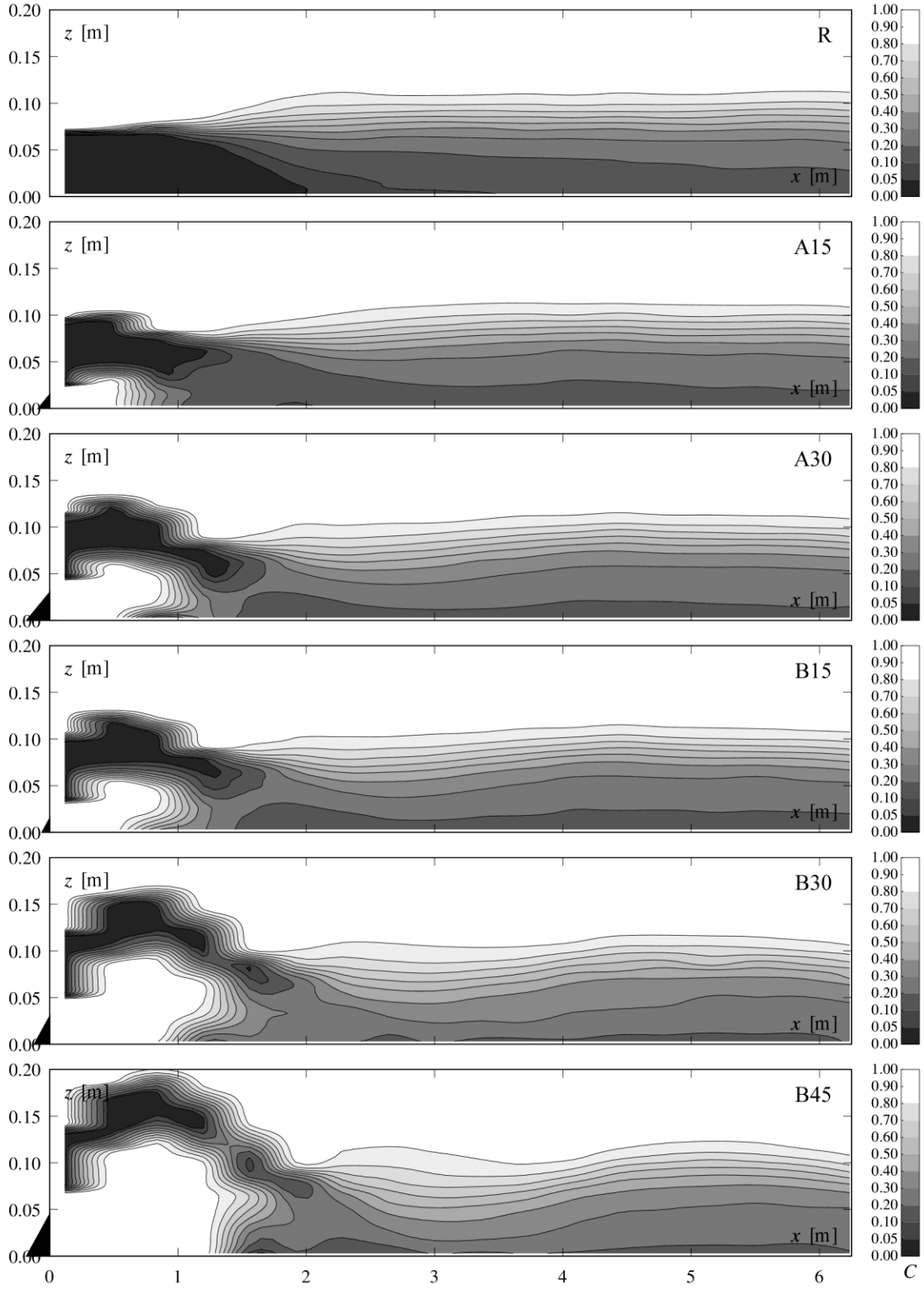

Figure 3. Contour plots of the air concentration $C(x, z)$ for reference test R without aerator, and tests A15, A30, B15, B30, and B45 with aerator (cf. Table 1)

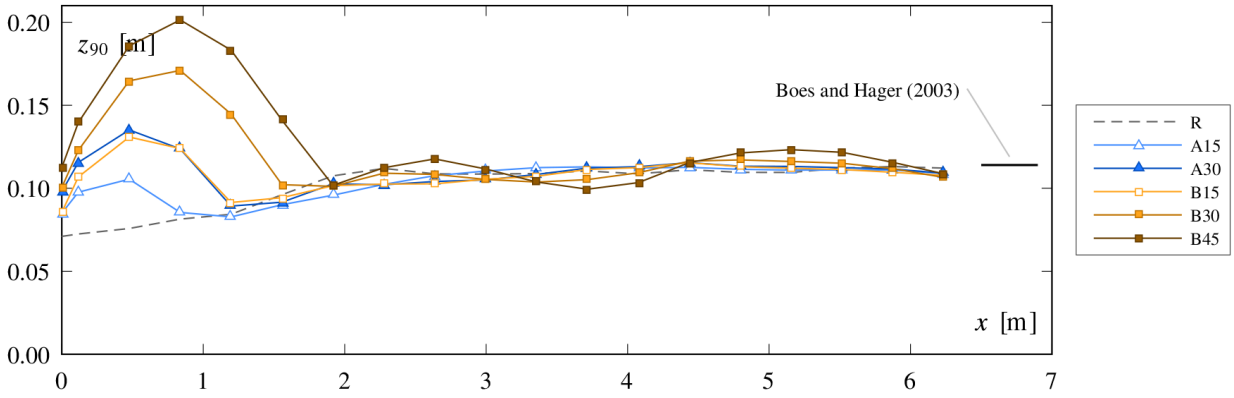

Figure 4. Water surface elevation z_{90} for the performed tests compared with uniform flow value from Boes and Hager (2003) (cf. Table 1 for test characteristics)

3.2. Air Entrainment Coefficient

The air entrainment coefficient $\beta = q_A/q$ increases with the deflector angle α and the deflector height t. This effect is directly linked to the increase of the jet length L (Figure 5). The relation $\beta = 0.0076L/h_o$ ($r^2 = 0.983$) is only valid for the specific φ, F_o and h_o tested herein and with negligible cavity subpressure. Deflector A30 and B15 coincidentally have about the same jet length and, therefore, a similar air entrainment coefficient.

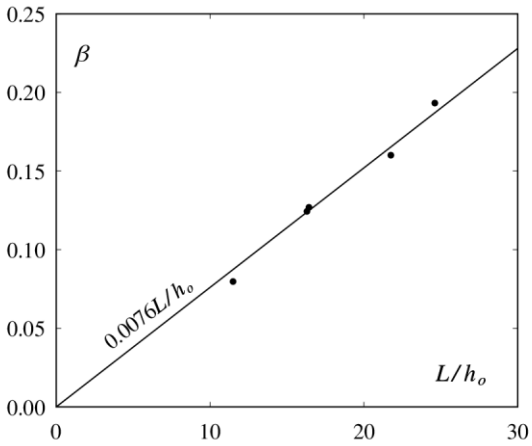

Figure 5. Air entrainment coefficient β as a function of the relative jet length L/h_o

3.3. Average Air Concentration

The average air concentration C_a is obtained by integrating the local air concentration from the bottom to z_{90} (lower surface z_{90} instead of the bottom for the jet) according to the definition of Straub and Anderson (1958). The streamwise development of C_a is shown in Figure 6. The value $C_a > 0$ at $x = 0$ m is due to the pronounced concentration gradient at the surface and the measurement technique. The average air concentration is obtained by integrating the air concentration profile with a linear interpolation between the measured points. This artificially adds air close to the surface. For aerated tests, there are two surfaces, and, therefore, the initial C_a is twice the value of the reference test R.

The development of the average air concentration in the jet is nearly identical for all aerated tests. The value decreases to a minimum at around $x = L$. The decrease is negligible for test A15, but the profile spacing might not be

able to accurately detect the maximum attained in the jet or the minimum at the jet impact. Then, the average air concentration increases again and reaches a maximum. This maximum is linked to the reflection of the jet on the steps. Series A and B both show an increase of the maximum with the increase of the deflector height t. The maximum also increases with the deflector angle α. Finally, the average air concentration stabilizes for all tests and converges to $C_a \approx 0.40$.

The uniform flow average air concentration for stepped chutes is the same as for smooth chutes (Boes 2000; Matos 2000). The values attained at the end of the channel compare well to Hager (1991), Chanson (1993), and Wilhelms and Gulliver (2005). A good agreement is also found for the indirect relation of Boes and Hager (2003) for stepped chutes, as suggested by Matos (2005).

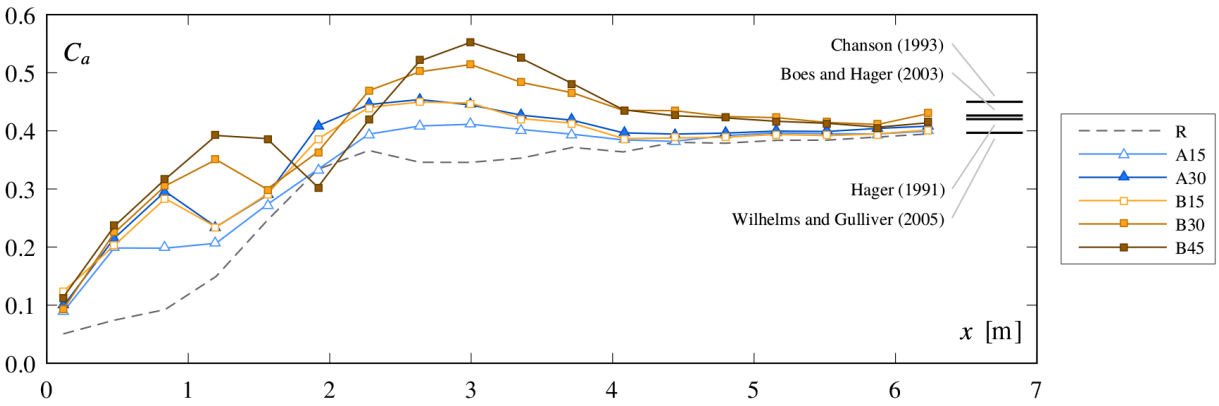

Figure 6. Average streamwise air concentration C_a development for the performed tests compared with uniform flow values according to different authors (cf. Table 1 for test characteristics)

3.4. Bottom Air Concentration

To protect the chute against cavitation, a bottom concentration above some percent is required where cavitation potentially occurs (Peterka 1953; Rasmussen 1956; Russell and Sheehan 1974). For the reference test R, the bottom inception point defined by $C_b = 0.01$ occurs at $x = 1.52$ m (Figure 7). The bottom air concentration then increases and reaches a value around $C_b = 0.15$ at the end of the channel.

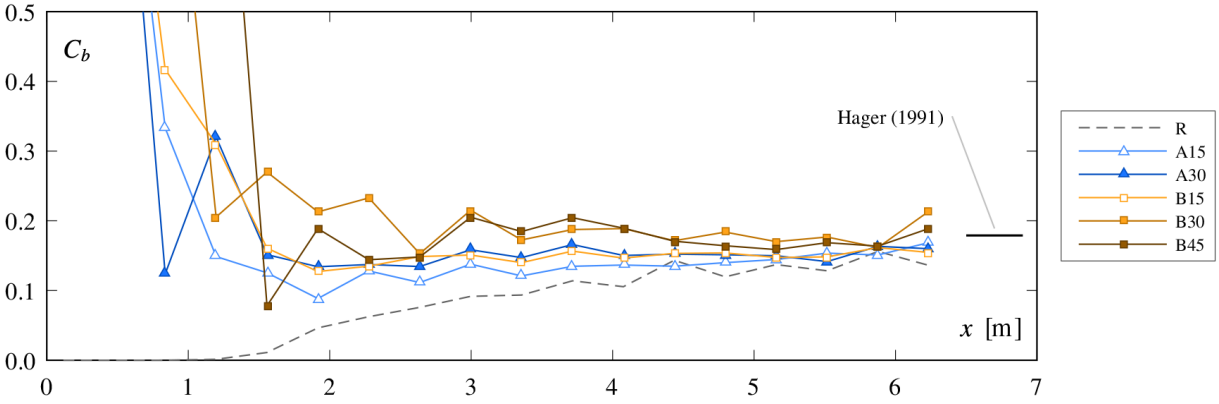

Figure 7. Streamwise bottom air concentration C_b development for the performed tests compared with uniform flow value for smooth chute (Hager 1991) (cf. Table 1 for test characteristics)

Tests with an aerator all follow the same trend, with a streamwise offset due to different jet lengths. At the beginning, while the flow is lifted off the bottom, the bottom air concentration is by definition $C_b = 1$ (air). The bottom air concentration rapidly decreases at the jet impact as water is encountered. Immediately before the impact, a minimum occurs – especially for tests A30 and B45 – as the roller is encountered. The roller velocity is low comparted to the jet velocity, and air is rapidly detrained as a consequence of the low turbulence. No cavitation can occur here due to the low velocity. For tests A15 and B15, there is no distinctive roller drop, which can be explained by a smaller roller or the absence of a profile in the roller. After the jet impact, the bottom air concentration rapidly attains an almost constant value. This value appears to be proportional to the jet length, as longer jets have a higher average air concentration. All tests then converge to a value around $C_b = 0.16$ at the end of the channel. It is interesting to note that C_b is close from the uniform flow value of $C_b = 0.18$ predicted by Hager (1991) for smooth chutes.

The good agreement of z_{90}, C_a and C_b with respective uniform flow values indicates that quasi-uniform flow state was reached at the end of the channel.

3.5. Air Concentration Profiles

Air concentration profiles in the middle ($x = 3$ m) and at the end ($x = 6.24$ m) of the channel are compared in Figure 8. In the middle of the channel, there is more air entrained for longer jets as previously observed for the air entrainment coefficient. At the end of the channel, all the profiles are nearly identical, with some differences close to the bottom.

The profile of test A15 changes very little between $x = 3.00$ m and $x = 6.24$ m, with some slight air detrainment on the upper half. This indicates that the reference test entrains more air towards the bottom on the second half of the channel, while tests A30, B15, B30, and B45 are subject to detrainment on the whole depth of the profile. Above the surface ($Z > 1$) for $x = 3.00$ m, tests B30 and B45 have a lower concentration, revealing that at this location there is more spray.

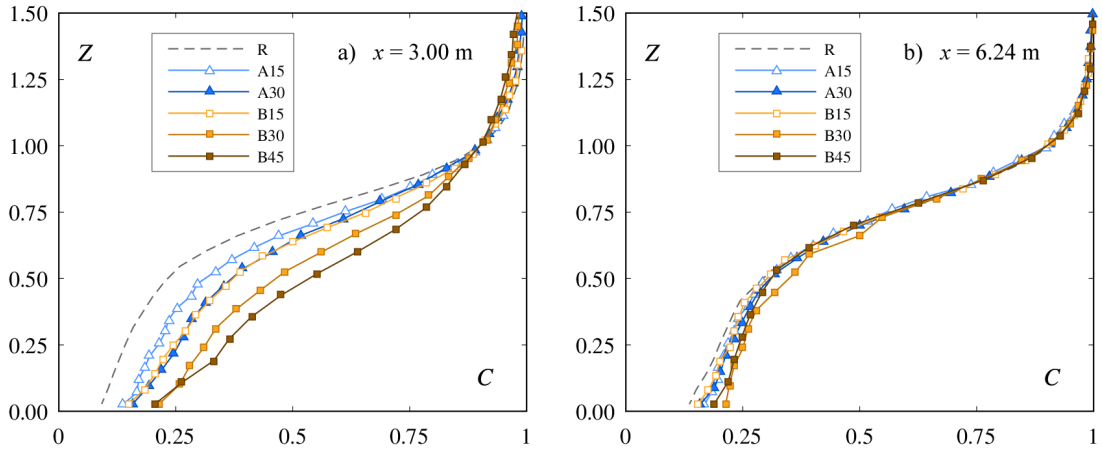

Figure 8. Air concentration profiles with $Z = z/z_{90}$ (cf. Table 1 for test characteristics)

4. CONCLUSIONS

An aerator consisting of a deflector and an air duct was placed at the transition between a smooth bottom chute and a stepped chute (end of ogee crest on a dam). Different deflector geometries as well as a reference set-up without aerator were tested for identical flow and chute conditions. Besides the jet, the surface perturbations downstream are small, and the jet impact generates spray. Quasi-uniform flow conditions are attained after $x \approx 3$–$5L$.

The major difference between the deflectors tested is the jet length, which has a direct and linear influence on the air entrainment coefficient β. After the jet impact, the bottom air concentration is close to or above the uniform flow value. Note that the minimum deflector angle tested was α = 9.46 °, and a flatter deflector might lead to smaller bottom air concentration. The bottom air concentration is above a few percent as recommended to protect against cavitation damages.

The smallest deflector, A15 with α = 9.46 ° and t/h_o = 0.2, shows an adequate air entrainment rapidly tending to uniform flow with minimal surface perturbation. Steeper or higher deflectors entrain more air that is rapidly detrained after the jet impact. Deflector A15 is an optimal deflector for the specific conditions tested (chute angle φ = 50 °, step height of s/h_o = 0.8, and approach flow Froude number F_o = 5.5). Other chute or flow parameters were not presented in this paper and change the effect of the deflector geometry.

5. ACKNOWLEDGMENTS

This research is funded by the Swiss National Science Foundation SNSF Grant No. 200021_137572/1 and the Lombardi Foundation.

6. REFERENCES

Amador, A., Sánchez-Juny, M., and Dolz, J. (2009). "Developing flow region and pressure fluctuations on steeply sloping stepped spillways." *Journal of Hydraulic Engineering*, 135(12), 1092–1100.

Boes, R. M. (2000). *Zweiphasenströmung und Energieumsetzung an Grosskaskaden*. VAW Mitteilungen 166, ETH Zürich.

Boes, R. M., and Hager, W. H. (2003). "Hydraulic design of stepped spillways." *Journal of Hydraulic Engineering*, 129(9), 671–679.

Chanson, H. (1988). "Study of air entrainment and aeration devices on a spillway model." University of Canterbury, New Zealand.

Chanson, H. (1993). "Self-aerated flows on chutes and spillways." *Journal of Hydraulic Engineering*, 119(2), 220–243.

Chanson, H. (2015). "Discussion of 'Cavitation potential of flow on stepped spillways' by K. Warren Frizell, F. M. Renna, and J. Matos." *Journal of Hydraulic Engineering*, 141(5), 07014025.

Falvey, H. T. (1990). *Cavitation in chutes and spillways*. Engineering monographs 42, U.S. Dept. of the Interior, Bureau of Reclamation, Denver, Colorado.

Frizell, K. W., Renna, F. M., and Matos, J. (2013). "Cavitation potential of flow on stepped spillways." *Journal of Hydraulic Engineering*, 139(6), 630–636.

Hager, W. H. (1991). "Uniform aerated chute flow." *Journal of Hydraulic Engineering*, 117(4), 528–533.

Kökpinar, M. A., and Göğüş, M. (2002). "High-speed jet flows over spillway aerators." *Canadian Journal of Civil Engineering*, 29(6), 885–898.

Koschitzky, H.-P. (1987). *Dimensionierungskonzept für Sohlbelüfter in Schussrinnen zur Vermeidung von Kavitationsschäden*. Mitteilung 65, Institut für Wasserbau, TU Stuttgart.

Kramer, K. (2004). *Development of aerated chute flow*. VAW Mitteilungen 183, ETH Zürich.

Matos, J. (2000). "Discussion of 'Characteristics of skimming flow over stepped spillways' by M. R. Chamani and N. Rajaratnam." *Journal of Hydraulic Engineering*, 126(11), 865–869.

Matos, J. (2005). "Discussion of 'Hydraulic design of stepped spillways' by R. M. Boes and W. H. Hager." *Journal of Hydraulic Engineering*, 131(6), 525–527.

Peterka, A. J. (1953). "The effect of entrained air on cavitation pitting." *Proc., Minnesota International Hydraulic Convention*, ASCE, New York, Minneapolis, 507–518.

Pfister, M. (2008). *Schussrinnenbelüfter Lufttransport ausgelöst durch interne Abflussstruktur*. VAW Mitteilungen 203, ETH Zürich.

Pfister, M. (2011). “Chute aerators: steep deflectors and cavity subpressure.” *Journal of Hydraulic Engineering*, 137(10), 1208–1215.

Pfister, M., and Boes, R. (2014). “Discussion of ‘Skimming, nonaerated flow on stepped spillways over roller compacted concrete dams’ by I. Meireles, F. Renna, J. Matos, and F. Bombardelli.” *Journal of Hydraulic Engineering*, 140(10), 07014012.

Pfister, M., and Chanson, H. (2014). “Two-phase air-water flows: Scale effects in physical modeling.” *Journal of Hydrodynamics, Ser. B*, 26(2), 291–298.

Pfister, M., Hager, W. H., and Minor, H.-E. (2006a). “Bottom aeration of stepped spillways.” *Journal of Hydraulic Engineering*, 132(8), 850–853.

Pfister, M., Hager, W. H., and Minor, H.-E. (2006b). “Stepped chutes: Pre-aeration and spray reduction.” *International Journal of Multiphase Flow*, 32(2), 269–284.

Rasmussen, R. E. H. (1956). “Some experiments on cavitation erosion in water mixed with air.” *Proc., International Symposium on Cavitation in Hydrodynamics*, National Physical Laboratory, London, 1–25.

Russell, S. O., and Sheehan, G. J. (1974). “Effect of entrained air on cavitation damage.” *Canadian Journal of Civil Engineering*, 1(1), 97–107.

Rutschmann, P. (1988). *Belüftungseinbauten in Schussrinnen*. VAW Mitteilungen 97, ETH Zürich.

Schiess Zamora, A., Pfister, M., Hager, W. H., and Minor, H.-E. (2008). “Hydraulic performance of step aerator.” *Journal of Hydraulic Engineering*, 134(2), 127–134.

Skripalle, J. (1994). *Zwangsbelüftung von Hochgeschwindigkeitsströmungen an zurückspringenden Stufen im Wasserbau*. Mitteilung 124, Technische Universität, Berlin, Germany.

Straub, L. G., and Anderson, A. G. (1958). “Self-aerated flow in open channels.” *Journal of the Hydraulics Division*, 84(7), 456–486.

Tan, T. P. (1984). *Model Studies of Aerators on Spillways*. Research report 84-6, University of Canterbury, Christchurch, New Zealand.

Terrier, S., Pfister, M., and Schleiss, A. J. (2015). “Comparison of chute aerator effect on stepped and smooth spillways.” *Proc., 36th IAHR Congress*, The Hague, The Netherlands.

Wilhelms, S. C., and Gulliver, J. S. (2005). “Bubbles and waves description of self-aerated spillway flow.” *Journal of Hydraulic Research*, 43(5), 522–531.